Materials & Design 214 (2022) 110425

Contents lists available at ScienceDirect

Materials & Design

journal homepage: www.elsevier.com/locate/matdes

Design of new modular metal pallets: Experimental validation and life cycle analysis

Enrico Zacchei [a], António Tadeu [a,b,*], João Almeida [a,c], Miguel Esteves [a], Maria Inês Santos [a], Samuel Silva [d]

[a] Itecons - Institute for Research and Technological Development in Construction, Energy, Environment and Sustainability, Rua Pedro Hispano s/n, 3030-289 Coimbra, Portugal
[b] ADAI-LAETA, Department of Civil Engineering, Faculty of Sciences and Technology, University of Coimbra, Pólo II, Rua Luís Reis Santos, 3030-788 Coimbra, Portugal
[c] Chemistry Centre, Department of Chemistry, University of Coimbra, 3004-535 Coimbra, Portugal
[d] Portimpact, Rua Zona Industrial 1080, 4580-565 Lordelo PRD, Portugal

HIGHLIGHTS

- New modular metal pallets that combine blocks and deck boards are proposed.
- 3D FEM, analytical, and experimental tests are carried out and results compared.
- More reliable values for loadings and displacements are provided for steel pallets.
- A comparative LCA suggests that steel pallets have a good environmental performance.

GRAPHICAL ABSTRACT

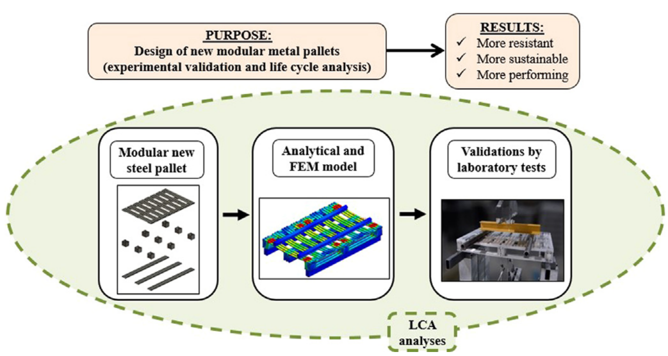

ARTICLE INFO

Article history:
Received 1 October 2021
Revised 8 January 2022
Accepted 24 January 2022
Available online 28 January 2022

Keywords:
Steel pallet
Pallet design
Experimental tests
Numerical analyses
LCA

ABSTRACT

Given the huge number of products transported worldwide every day, it would be advantageous to use lightweight pallets made of readily recyclable materials that are easy to clean, durable, and cheap to maintain. However, the design process for new metal pallets does not follow any specific code, which makes the transition to products with improved characteristics more challenging. This paper describes the development of a new modular steel pallet that combines blocks and deck boards to produce a range of configurable geometries for use in transportation (forklifting) and stationary (racking, stacking) conditions alike. Analytical and numerical analyses using the 3D finite element method (FEM) were carried out. Experimental tests were performed to evaluate ultimate strengths and deformations for different loadings. The experimental results used to validate the numerical models showed that these pallets performed well in terms of stiffness, deformation, and stresses. A comparative life cycle analysis (LCA) was also carried out to identify the main environmental impacts of the life cycle of pallets made from different materials. The results of a "cradle-to-gate with options" model suggest that the new proposed pallet performs better than its wood, plastic, and aluminium counterparts.

1. Introduction

World merchandise trade has grown tenfold in the last 30 years and accounts for more than half of the total world economy [1]. Pallets are the most used unit-load portable platform in the global market since goods can be moved and transported very efficiently

* Corresponding author.
E-mail addresses: enrico.zacchei@itecons.uc.pt (E. Zacchei), tadeu@itecons.uc.pt (A. Tadeu), joao.almeida@itecons.uc.pt (J. Almeida), miguel.esteves@itecons.uc.pt (M. Esteves), mariaines.santos@itecons.uc.pt (M.I. Santos), samuel.silva@portimpact.com (S. Silva).

https://doi.org/10.1016/j.matdes.2022.110425
0264-1275/

and reliably using standard devices. Without pallets, goods would have to be either lifted manually or moved using more complex equipment, thus increasing handling costs [2]; as mentioned by the National Wooden Pallet and Container Association [3] "pallets move the world". Also, pallets are particularly relevant, for instance, in the air transport of different products [4].

Different types of pallets are available to meet various loading requirements, costs, and other specific prerequisites. Pallets can be made of materials such as solid wood, softwood [6], plastic, paper, recycled paper, corrugated paperboard, metal, wood-based composites, and wood-plastic [5,7]. Of these, wooden and plastic pallets are the most popular [8,9].

Pallet design, including choice of materials, must ensure the ability to withstand several loading cycles. However, pallet damage is inevitable after a certain number of uses, which means that a high recyclability rate that enables the easy reuse of discarded parts should be considered [10,11]. The environmental impacts generated by the wrong use, or the non-reuse of pallets have been addressed by different authors [1,12]. There are also papers on the environmental impact of pallet remanufacturing operations and logistic systems, as well as on evaluating the performance of the pallet's structural design [13,14].

Several LCA studies have focused on comparing different life cycle stages, analysing details such as materials used, transported loads [19], number of trips made, reuse rates, repair and treatment needs, and end of life processes [16,18]. However, to the best of the authors' knowledge, there are no LCA studies on aluminium and galvanised steel pallets. Plastic pallets have typically greater impact on the product stage than wooden pallets. However, their durability is expected to be greater, diluting the impact over the life cycle [20,22]. Repairing and reusing wooden pallets is a good strategy to increase their lifespan and reduce their environmental impact throughout the life cycle [24,25].

In terms of design, although Eurocodes EN 1993-1-3 [26] and EN 1993-1-1 [27] may be applied, depending on the material used and the structures, no structural calculation and verification method is explicitly for metal pallets. The methods used to verify pallet design and manufacture are empirical and based mainly on experimental testing [29]. Some analytical equations are shown in [35] but only for pallet separators/stoppers. In this context, some researchers have focused on the so-called "pallet loading problem" (PLP) [30,31], studying the multi-pallet loading in terms of load positions and magnitude with the aim of optimising the number of pallets needed [14] and the possible multiple levels of pallet loadings [12].

After a comprehensive review of the literature, the authors have not found significant studies specifically about modular metal pallets. Thus, papers on other structures similar to pallets have also been analysed (e.g. stringer pallets [32,33], panel deck pallets, pallet beams [34], steel pallet racks [36]). In this regard, it is possible to find approaches for steel pallet racks that can be used in the design of new metal pallets. For instance, [36] discusses the design and performance of steel pallet racks, in [37] the prediction of their strength is estimated, and in [38] the beam-to-column connection is treated.

In this work, the authors address the development of steel pallets with configurable modular components using a technology that enables the pallets to be easily assembled. New data is provided for pallet design by focusing on the development of 3D models.

The following goals were defined:

(i) to analyse pallets made of different materials, including those made of metal, in terms of relevant technical, economic and environmental factors;
(ii) to propose a new modular steel pallet with high functional value;
(iii) to rationalise the behaviour of individual structural components (blocks and deck boards) and the entire pallet;
(iv) to validate the design of the new pallet with laboratory tests; and
(v) to carry out a life cycle analysis, comparing the environmental performance of the new proposed pallet with those made of wood, plastic or aluminium.

The methodology used comprised three main steps. Firstly, the modular pallet was designed, the structural schemes (i.e. forklifting, racking, stacking) defined, and the materials selected. Analytical solutions [40], analysis using Eurocodes [26,27], and numerical analyses via the finite element method (FEM) [39] were carried out. Then, the mechanical behaviour was validated by performing laboratory tests required by the prevailing international standards ISO 8611-1 [41], ISO 8611-2 [42] and ISO 8611-3 [43]. Ultimate and test loads were quantified in this step. Finally, an LCA was performed to assess the environmental performance of the new proposed pallet over the life cycle.

2. Conceptualisation of modular metal pallets

In general terms, a pallet's performance is strongly related to the physical properties of the used raw material. Thus, a comparative analysis of wood, plastic, paper, and metal pallets was carried out based on a set of factors often used to determine the pallet's suitability for a given application. For this purpose, several mechanical (resistance, stiffness, weight) and socio-economic (durability/lifespan, cost, sustainability, use) parameters have been collected from the literature. Additionally, for simplicity, performance was qualitatively rated as weak, satisfactory, or good. According to this comparative evaluation, presented in Table 1, metal pallets perform better in terms of durability, mechanical resistance, stiffness, and lifespan. However, they tend to be more expensive and heavier.

In terms of size, pallets of 1200 mm $\times$ 800 mm, known as the Euro or Universal pallets, are very common in Europe. In Asia, 1100 mm $\times$ 1100 mm is the most widely used pallet size, whereas pallets measuring 1219 mm $\times$ 1016 mm are used in the USA [2].

The new modular welded steel pallet under study is formed of 8 transverse deck boards (800 mm $\times$ 120 mm), 3 longitudinal bottom deck boards (1200 mm $\times$ 120 mm), 3 longitudinal top deck boards (1200 mm $\times$ 120 mm), and 9 cubic blocks (1 at each corner, 1 halfway along each side, and 1 in the centre) 96.2 mm wide (see Fig. 1).

This pallet is considered modular since its components are interchangeable with each other and are removable. This is possible since the deck profiles have a common geometry that can be connected to the block elements.

Cold-formed steel DX51D was selected to build the pallets since it is often used in similar support structure applications (Table 2 lists its main properties [49,50]).

The model design is based on the testing setups used for laboratory evaluation, as given in the literature [41,42,43,51,52]. In particular, the experimental test procedure for evaluating new flat pallets for material handling is specified in ISO 8611-1 [41]. The test method is divided into groups for nominal load testing, maximum working load testing and durability comparison testing. ISO 8611-2 [42] gives the performance requirements to establish nominal loads for new pallets, defines the tests required in various handling environments and states the performance requirements for the tests with payloads. Finally, ISO 8611-3 [43] defines how the maximum working load for pallets with known payloads is determined for different handling environments [46].

Table 1
Comparative evaluation of pallets made of different materials.

Factor	Wood [a]	Plastic [b]	Paper [c]	Metal [d]
Cost [8,15,44,45,46]	***	*	**	*
Durability/lifespan [8,44,45,46,47]	*	***	*	***
Mechanical resistance [44,45,46,47]	*	***	*	***
Stiffness [8,45,46,47]	N/A	*	*	***
Sustainability [8,29,44,45,46]	**	*	***	**
Use [4,6,8,45,47,48]	***	***	*	*
Weight [8,15,44,45,46]	*	***	***	*

Note: * = Weak. ** = Satisfactory. *** = Good. N/A = Not available.
[a] It includes solid wood, softwood, composite wood-plastic (wood + polymeric materials), composite wood and paperboard wood.
[b] High-density polyethylene reinforced plastic, polyethylene terephthalate reinforced plastic and resin formulations.
[c] Corrugated, honeycomb, solid fibreboard, and moulded pulp.
[d] Carbon steel, stainless steel, and aluminium.

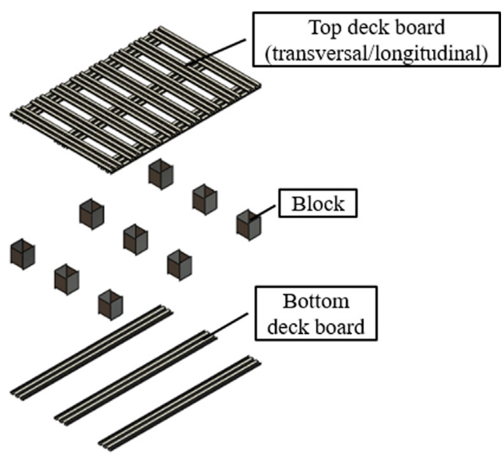

Fig. 1. Assembly of the metal pallet: 8 transverse deck boards and 3 longitudinal top deck boards (top image), 9 cubic blocks (middle), 3 longitudinal bottom deck boards (bottom).

Table 2
Mechanical and geometrical properties [27,49].

Yield strength, f_y (MPa)	Tensile strength (MPa)	Elastic modulus, E (GPa)	Poisson's ratio
140.0	From 270.0 to 500.0	210.0	0.30
Mass density (kg/m^3)	Deck boards mass (kg)	Block mass (kg)	Pallet mass (kg)
7850.0	11.25	0.29	13.86 (=11.25 + (9 × 0.29))

Three different static tests need to be performed to simulate real loading conditions:

(1) The stacking test simulates compressive loads by placing pallets on top of one another without intermediate shelves.
(2) The racking test simulates the storage of unit compressive loads in drive-in or beam racks with free unsupported spans.
(3) The forklifting test simulates the shock and impact force through the load carried by the pallet in moving use.

The forklifting test can be seen as a "dynamic" test due to the impact force of the moving supports [52] therefore, in this work a dynamic fatigue test has been also carried out.

Fig. 2 illustrates the three tests in longitudinal and transverse view of the whole system (i.e. pallet + supports + external loads) as explained below.

- Grey elements: transverse/longitudinal deck boards and blocks that form the whole metal pallet with the geometrical and mechanical characteristics already mentioned.
- Turquoise elements: mechanical restraints where the reaction forces are developed to equilibrate the whole system. They are represented by metallic elements with rectangular hollow sections of ~1.50 m. In the forklifting test they simulate the fork supports, whereas in the racking test they simulate beam racks for storage. In the stacking test, they are coincident with the contact points between the longitudinal bottom deck boards and the ground.
- Orange elements: the gravity loadings are represented by metallic elements with circular hollow sections of ~1.50 m. For the forklifting tests, square hollow sections of ~1.50 m and rectangular section of ~1.0 m are also used. The total weight of these elements ranges between 150.0 and 670.0 N.

All loads and reactions are assumed to be vertical. All listed loading conditions are intended to assist the designer in establishing an acceptable initial compromise between the cost and performance of these products.

ISO 8611-2 [42] provides some examples of ultimate loads (U_t) and test loads (P_t) defined by 50% of U_t. These U_t loadings are 28.40 kN, 35.0 kN, 44.20 kN for racking, forklifting, and stacking, respectively. These values have been used as reference to analyse the proposed steel pallet.

3. Design and FEM modelling

The purpose of the structural analysis is to evaluate the flexural strength of the decks and the compressive strength of the blocks to estimate the pallet's maximum load capacity in accordance with Eurocode 3 [26,27,28].

3.1. Structural components

As the structural components (blocks and deck boards) of the pallet are cold-formed steel profiles, the effective cross-section is based on the effective areas of the compression elements $A_{c,eff}$, and the effective area of the tension elements to shear lag [27]. $A_{c,eff}$ is defined in accordance with Eurocode 3 [28] as:

$$A_{c,eff} = \rho A_c, \quad (1)$$

where A_c is the gross cross-sectional area and ρ is the reduction factor due to plate buckling. The plate buckling effects caused by stresses at the ultimate limit state (ULS) need to be taken into account, considering that:

- the panels are rectangular, and flanges are parallel;
- there are stiffeners in the longitudinal/transverse direction;

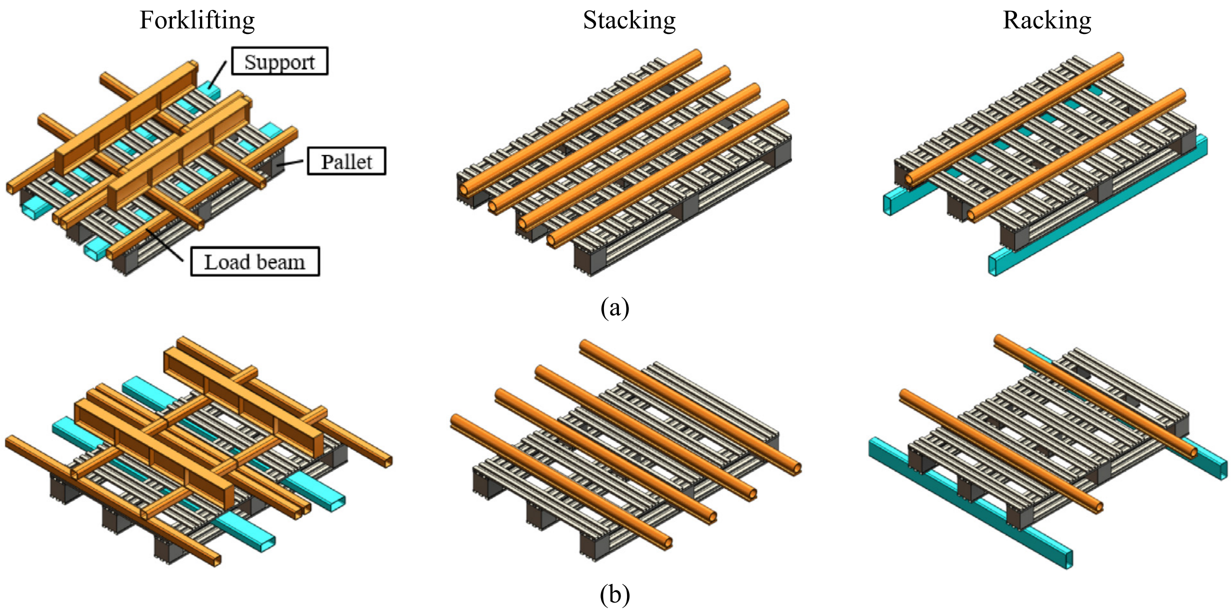

Fig. 2. Illustrations of the experimental tests in (a) transverse and (b) longitudinal side. The metal pallet is grey, load beams are orange, and supports turquoise. (For interpretation of the references to colour in this figure legend, the reader is referred to the web version of this article.)

– open holes and cut-outs are small;
– members have uniform cross-section;
– no flange-induced web buckling occurs.

For internal compression elements, the parameter ρ can be computed as follows [28]:

$$\begin{cases} \rho = 1.0 & for \ \bar{\lambda}_p \leq 0.5 + \sqrt{0.085 - 0.055\psi} \\ \rho = \frac{\bar{\lambda}_p - 0.055(3+\psi)}{\bar{\lambda}_p{}^2} \leq 1.0 & for \ \bar{\lambda}_p > 0.5 + \sqrt{0.085 - 0.055\psi} \end{cases}, \tag{2}$$

with the plate slenderness, $\bar{\lambda}_p$, defined as:

$$\bar{\lambda}_p = \sqrt{\frac{f_y}{\sigma_{cr}}} = \frac{\bar{b}/t}{28.4\sqrt{\frac{235 \times k_\sigma}{f_y}}}, \tag{3}$$

where ψ is the stress ratio, $\bar{b}$ is the width of the lateral faces (of the blocks) and of the flanges and webs (for the deck boards), k_σ is the buckling factor, t is the plate thickness and σ_{cr} is the elastic critical plate buckling stress.

To define $A_{c,eff}$ using Eq. (1), the following iterative procedures should be implemented [26]: (i) the parameter ψ used to determine the effective width of flanges of a section subject to stress is based on gross section properties; (ii) ψ used to determine the effective width of the web is obtained using the $A_{c,eff}$ for flange and the gross area of the web; (iii) the effective section properties may be refined by applying ψ based on the effective cross-section already found in place of A_c.

3.2. Blocks of the pallets

Table 3 lists the parameters used to calculate the $A_{c,eff}$ subject to uniform compressive stresses. In this case, the parameter ψ is defined iteratively, given that the location of the gravity centre ($CG_{,c,eff}$) corresponds to the gravity centre ($CG_{,g}$) of A_c, as shown in Fig. 3. It can be concluded that when the blocks are subjected to uniform compression, the effective width of the lateral faces is 63.6% (ρ = 0.636).

Thus, the axial compression resistance of the block, $N_{c,Rd}$, is defined as:

$$N_{c,Rd} = A_{c,eff} \times f_y, \tag{4}$$

leading to $N_{c,Rd}$ = 34.27 kN, which represents a good value, given the expected load to be stacked on the pallets.

By considering that the proposed steel pallet consists of 9 blocks, it is possible to estimate that the compressive resistance of the whole pallet is 308.43 kN (=9 × 34.27 kN).

The FEM simulation of the block under this compressive load [39], with a fixed base, leads to the plotted von Mises stresses shown in Fig. 4. The obtained maximum stress of 87.77 MPa is lower than f_y = 140.0 MPa (see Table 2).

Eqs. (1)–(3) are from Eurocode [28], and they reduce the gross cross-sectional area of cold-form steel profiles under compressive loads, $A_{c,eff}$, accounting for the possible plate buckling phenomena. This reduction is specifically more relevant due to the low value of the yield strength, f_y: ρ ≤ 1.0 (since $\bar{\lambda}_p$ = 1.307 > 0.673) from Eq. (2) which leads to the reduction of A_c. This could be seen as a safer approach.

Table 3
Parameters defined for all lateral faces of the blocks under compressive loading.

	$\bar{b}$ (mm)	t (mm)	ψ	k_σ	$\bar{\lambda}_p$	ρ	Internal compression element	
							b_{eff} (mm)	$b_{e1} = b_{e2}$ (mm)
Lateral faces	96.20	1.0	1.0	4.0	1.307	0.636	61.20	30.603

Note: the effective width, b_{eff}, is defined by ρ × $\bar{b}$ and $b_{e1} = b_{e2} = 0.5\ b_{eff}$.

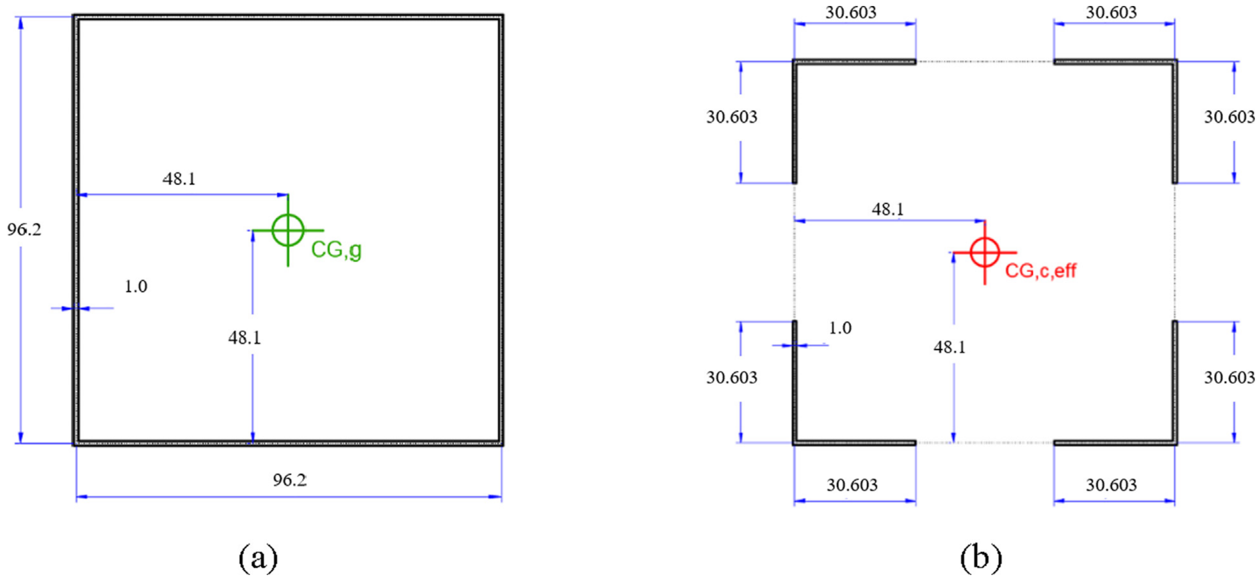

Fig. 3. Geometry of the cross-section of the blocks (dimensions in mm): (a) gross area A_c (384.90 mm^2); (b) effective area $A_{c,eff}$ (244.8 mm^2) [61].

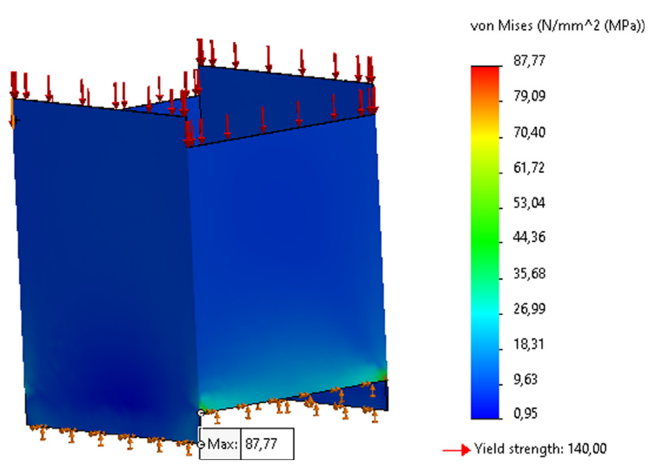

Fig. 4. Von Mises stresses in the block under a compressive load of 34.27 kN.

Indeed, this reduction underestimates $N_{c,Rd}$ (Eq. (4)). The numerical model results did not show the existence of a buckling phenomenon (see Fig. 4). A larger $N_{c,Rd}$ would be obtained using A_c as: $N_{c,Rd}$ = 384.90 mm^2 $\times$ 140.0 MPa = 53.88 kN $\rightarrow$ 9 $\times$ 53.88 kN = 484.92 kN.

3.3. Deck boards of the pallets

The following tables give the parameters used to calculate A_{eff} subjected to a positive (Table 4) and negative (Table 5) bending moment [53]. For deck boards, it is taken that ρ = 1.0 since $\bar{\lambda}_p \leq 0.673$ following Eq. (2).

Fig. 5 shows the A_{eff} of the transverse section of the deck boards when subjected to positive and negative bending flexure. In these cases, A_{eff} corresponds to the gross section since all components of the transverse section are effective.

The deck board is designed for elastic and elastic–plastic resistance with yielding at the compressed flange. The design moment resistance of a cross-section for bending in the horizontal axis ×, $M_{x,Rd}$, is determined as follows:

$$M_{x,Rd} = W_{x,eff} \times f_y, \tag{5}$$

where $W_{x,eff}$ is the effective section modulus calculated as $W_{x,eff} = I_{x,eff}/\upsilon$ with υ being the distance between the CG_g and the bottom flange. Table 6 shows the results of the transverse section design.

Assuming that the constant bending moment of 55.87 N × m is distributed along the simply supported deck board with a length of 800.0 mm, the following von Mises stresses are obtained (see Fig. 6). In terms of resistance design force, the value of 0.46 kN (=55.87/0.12) is obtained. The negative and positive maximum stresses are −127.0 MPa and 138.0 MPa, respectively. Both stresses are close to (but below) f_y = ±140.0 MPa.

3.4. Whole metal pallet

The 3D analyses of the global metal pallet were carried out using a numerical model in FEM elements [39]. The model was built using all blocks and deck boards to form the whole structure. Solid elements models were used for all components (i.e. deck

Table 4
Parameters defined for the flanges and webs of the boards under positive bending flexure.

	$\bar{b}$ (mm)	t (mm)	ψ	k_σ	$\bar{\lambda}_p$	ρ	Internal compression element		
							b_{eff} (mm)	b_{e1} (mm)	b_{e2} (mm)
Flanges	19.88	0.60	1.0	4.0	0.45	1.0	19.88	7.95	11.92
Webs	11.40 [a]	0.60	−1.18	28.41	0.097	1.0	5.23	2.09	3.13

Note: b_{eff} is the effective width defined by $(\rho \times \bar{b})/(1 - \psi)$. b_{e1} is the effective width subject to compressive stresses defined by 0.4 b_{eff} [28]. b_{e2} is the effective width subject to compressive stresses defined by 0.6 b_{eff} [28].
[a] The folded lengths used at the ends are 0.80 mm and 2.70 mm.

Table 5
Parameters defined for the flanges and webs of the boards under negative bending flexure.

	$\bar{b}$ (mm)	t (mm)	ψ	k_σ	$\bar{\lambda}_p$	ρ	Internal compression element		
							b_{eff} (mm)	b_{e1} (mm)	b_{e2} (mm)
Flanges	19.88	0.60	1.0	4.0	0.45	1.0	19.88	7.95	11.92
Webs	11.40	0.60	−0.85	20.17	0.115	1.0	6.16	2.47	3.69

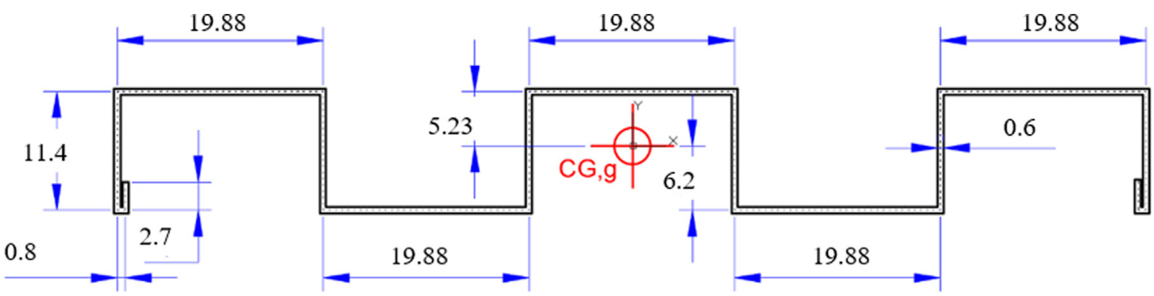

Fig. 5. A_{eff} of the transverse section for positive/negative flexure.

Table 6
Design moment resistance of the transverse section for positive/negative flexure.

A_{eff} (mm^2)	$I_{x,eff}$ (mm^4)	υ (mm)	$W_{x,eff}$ (mm^3)	$M_{x,Rd}$ (N × m)
105.3	2462.15	6.20	399.05	55.87

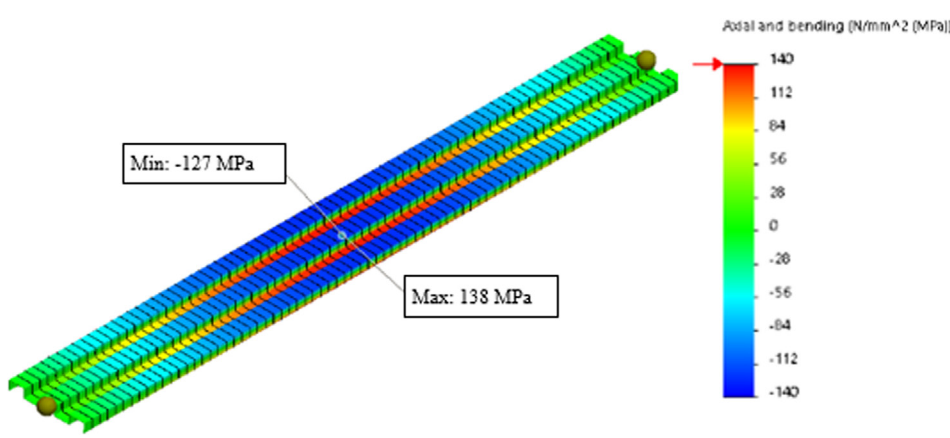

Fig. 6. Von Mises stresses obtained when a deck board with a length of 800.0 mm (800.0 mm × 120.0 mm) is loaded with a uniform bending moment of 55.87 N × m (design resistance: 55.87/0.12 = 0.46 kN).

boards, blocks, supports, load boards), assuming that the bases were fixed. For the racking and forklifting case, the fixed restraints coincide with the supports, whereas for the stacking case they coincide with the contact points between the deck boards and the ground.

Fig. 7 shows the von Mises stresses for all analysed cases when subjecting the pallets to the U_t loadings listed in Table 8.

Red (116.70–140.0 MPa) highlights the regions where the von Mises stresses are close to f_y. The racking tests yielded the most critical cases on both sides, while the forklifting test produces the most critical cases for the longitudinal side. In the other tests, the values range between 23.33 MPa (blue region) and 93.33 MPa (green region).

Expressive deflections are also noted (but not in scale), particularly for the racking case along the longitudinal side, which could be relevant to the design of the pallets, besides the strength. This aspect is discussed in Section 4.2, below.

4. Mechanical behaviour and validation tests

This section discusses the laboratory tests carried out to determine the mechanical behaviour of the whole steel pallet and its components. With this data, the numerical results already shown in previous sections could be completely validated and thus it should be possible to find a relationship between the pallet and structural components.

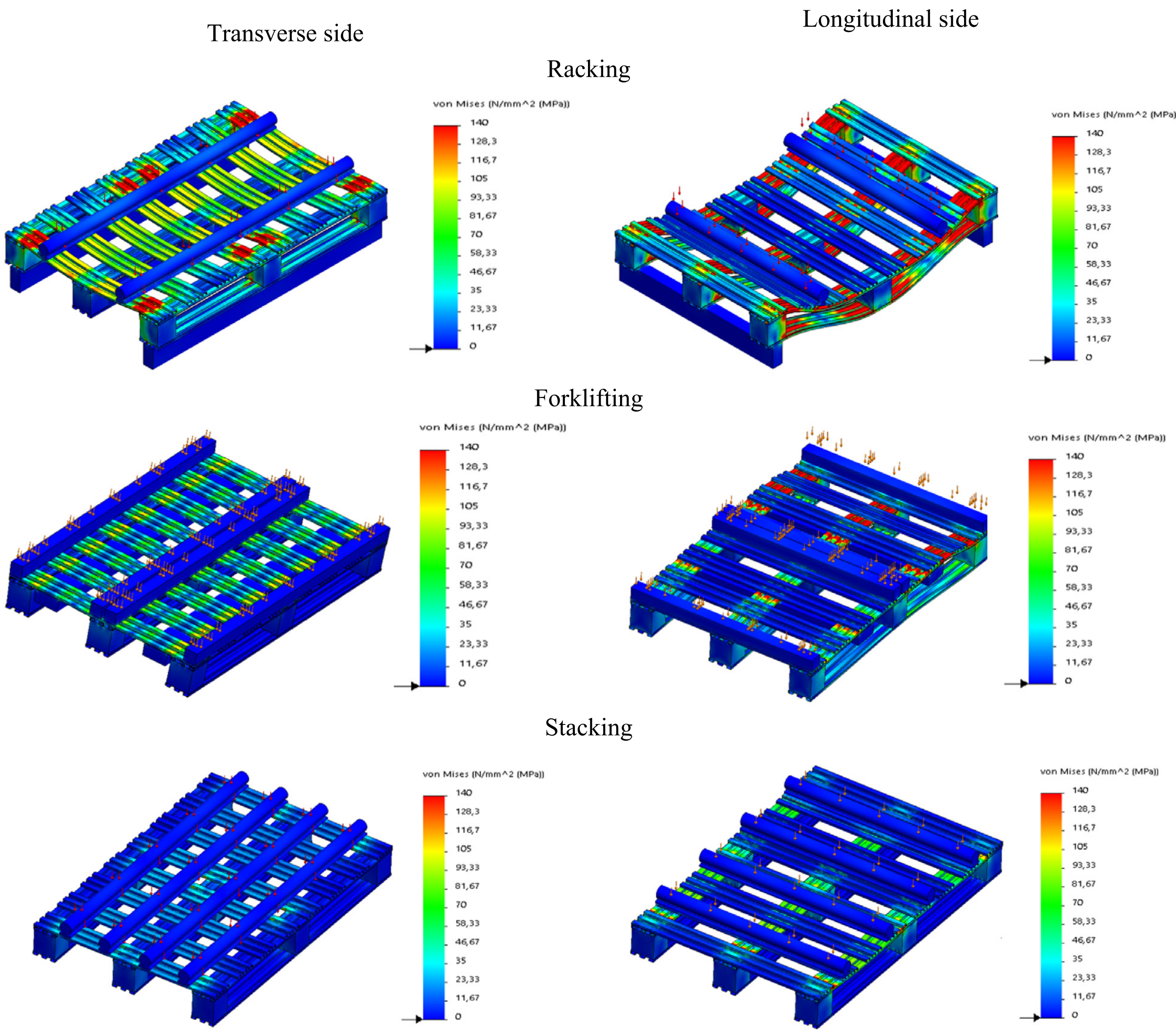

Fig. 7. Computational von Mises stresses under U_t loadings (see Table 8).

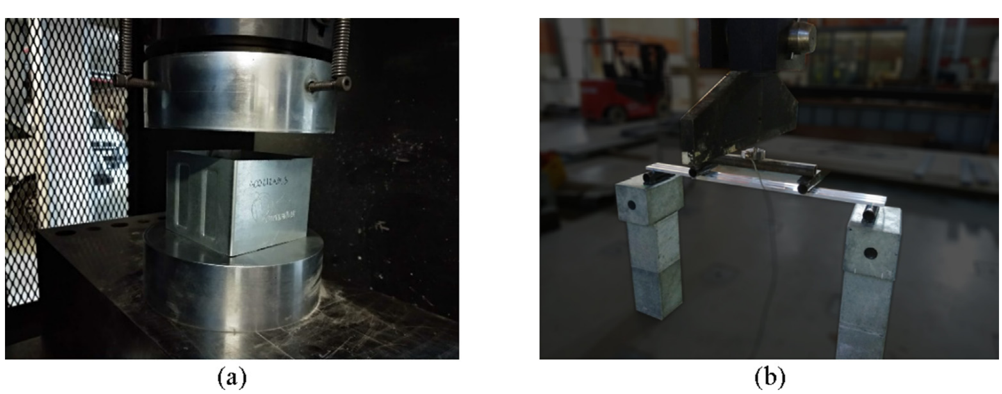

Fig. 8. Laboratory tests of the steel structural components: (a) block and (b) deck board.

4.1. Deck boards and blocks

Fig. 8 shows the images of the tests and the equipment used. For testing the blocks and deck boards, a compression testing machine from Instron (600 RD) with a 3.0 MN load cell, and a hydraulic actuator from Instron (Satec KN600K3965) with a 600 kN load cell were used, respectively.

LVDT transducers, model HBM type WAT-100, were used to measure the vertical displacements. Two HBM MX840 A/B data loggers set up with HBM Catman AP 4.03 software were used to collect the data [54]. All sensors were previously calibrated. All tests were carried out in the laboratory facilities of Itecons (Coimbra, Portugal).

Fig. 9 shows the results of the laboratory tests (6 tests) of the blocks and deck boards on the transverse (T-side) and longitudinal (L-side) sides. Results are shown by elasto-plastic load/displacement curves.

In Fig. 9(a), it is possible to see the ductile behaviour of the blocks since the curves do not strongly decrease after the peak point. However, the variability between the curves indicates the real difficulty when it comes to evaluating this type of element.

The experimental peak values of the block range between 43.61 and 55.95 kN, which are greater than the analytical values of 34.27–53. 88 kN, as expected following the explanations given in Section 3.2.

For the deck boards (Fig. 9(b)), the initial inclination of the curves (that is associated with the structural stiffness) and the peak values between the longitudinal and transverse deck boards are substantially different. For the longitudinal deck board, the mean peak value is 0.83 kN, which is 1.88 times smaller than that of the transverse deck board (i.e. 1.56 kN). As expected, both mean peaks reached satisfactory values, since they are greater than 0.46 kN (see Fig. 6).

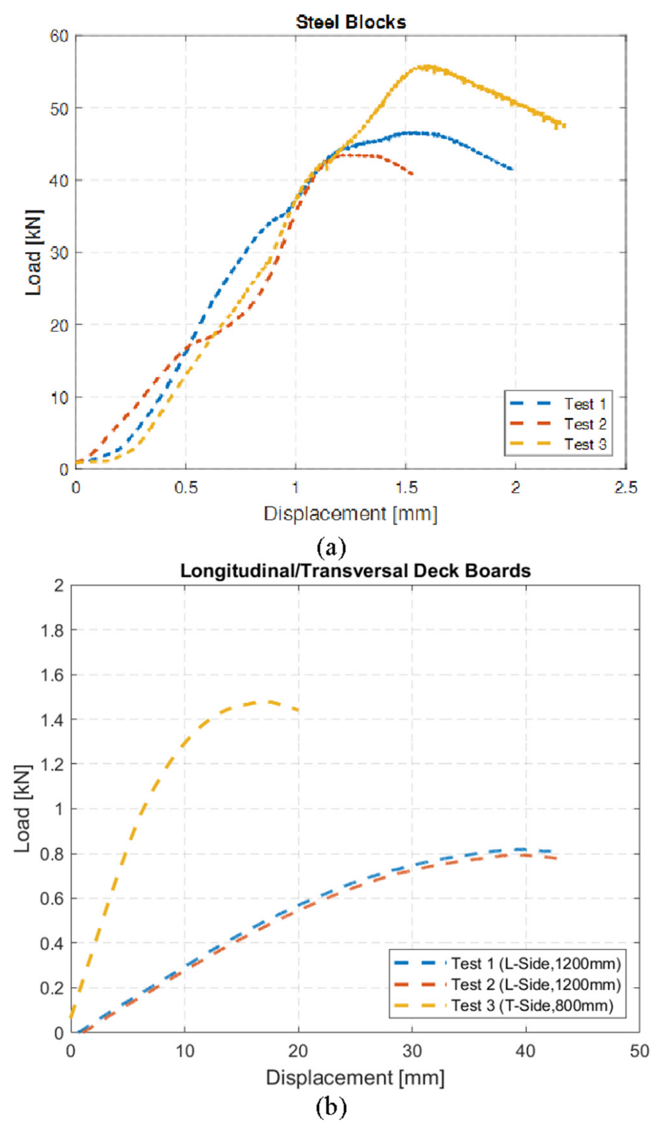

Fig. 9. Results of laboratory tests of the (a) blocks and (b) transverse and longitudinal deck boards.

4.2. Static behaviour of the whole pallet

The ultimate load for a total pallet failure, U_t, and the pallet load capacity, P_t, are estimated in this subsection.

The bending strength and bending stiffness can be defined from the test results [41,42,52].

ISO 8611-2 [42] defines P_t as the minimum weight of the load that corresponds to a prescribed deflection limit (or stiffness limit) and of that corresponding to U_t divided by a safety factor of 2.0 (i.e. flexural limit).

Fig. 10 shows photos illustrating the racking, forklifting, and stacking tests (for the two sides) consistent with the illustrations shown in Fig. 2. The equipment used was the same as that described for testing the deck boards in Section 4.1. This figure also highlights the positions of the LVDT transducers by including a schematic plot (red elements).

Table 7 shows the geometrical data used for the analysis, with l_i being the distance between the deck board supports and a_i the distance between the point where the load is applied and the closest deck board support.

The racking test determines U_t and P_t by focusing on the bending strength and bending stiffness. The maximum load capacity $P_{t,max}$ of the pallet is determined when the pallet is placed on supports on the transverse and longitudinal sides. $P_{t,max}$ is defined as a range between the minimum ultimate load $U_{t,min}$ of the first welding point failure, and the maximum ultimate load $U_{t,max}$ (divided by 2.0).

The limit condition of the forklifting test is the flexural bending of the pallet on fork supports under the top deck of the pallet. Here $P_{t,max}$ is determined when pallets are moved by load handling equipment on the transverse and longitudinal sides. For all pallet models, the minimum weights are obtained when the pallets are moved from the longitudinal side, because the ends of the pallets (which extend beyond the forks) are longer and thus subjected to greater stresses.

The stacking test determines the ability of the pallet top and bottom decks to withstand the local effects of widely varying payloads on sub-spans of decks between blocks in a block stacking situation. When pallets are stored by stacking, $U_{t,max}$ is determined by the strength of the upper deck and the lower deck. On the other hand, when there is no possibility of stacking the pallet's $U_{t,max}$ is determined only by the strength of the upper deck.

Preliminary experimental tests showed that failure happens with the loss of the welding joints. Thus, the pallet strength would increase if the quality and length of the welded joints were improved. All joints were improved by performing a continuous weld. The results of these tests are presented and discussed next.

Fig. 11 shows the load–displacement curves (solid lines) recorded during the laboratory tests for all cases on both sides. All tests are performed by loading the test specimen to reach a certain deformation (2% of the distance between supports in the case of the racking and stacking tests; 20 mm in the case of the forklifting tests), unloading, and then reloading up to failure. The numerical results (dashed lines), computed assuming elastic behaviour, are included for comparison.

The differences between the experimental and numerical curves quantify the real contribution of the material and the connection between pallet elements. The slopes of the numerical lines are similar to the slopes of the first part of the experimental curves, where the pallets maintain the elastic-linear behaviour.

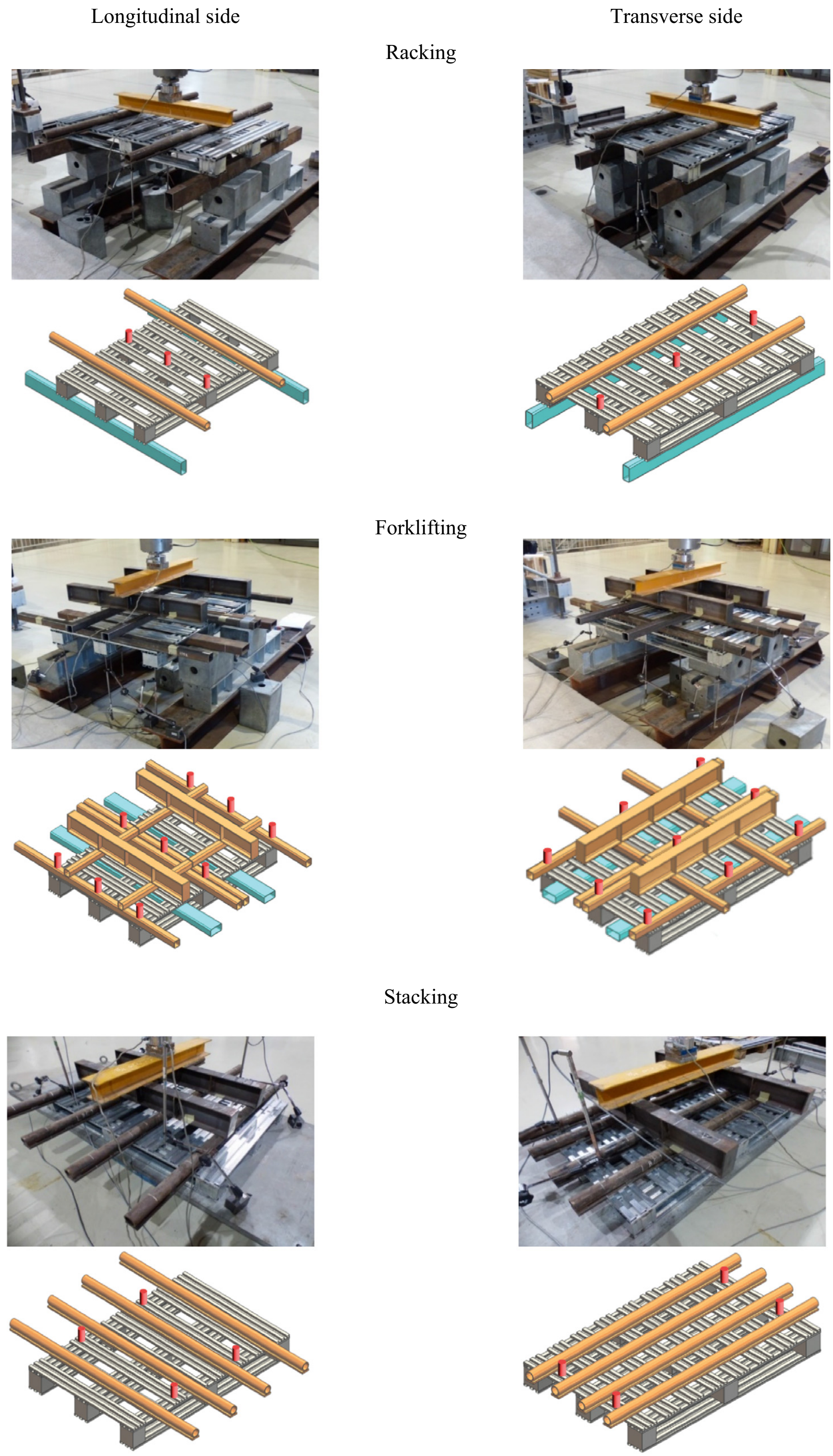

Fig. 10. Photos of the racking, forklifting, and stacking laboratory tests (from both sides).

Table 7
Geometric data for laboratory tests.

Parameter	Forklifting case		Stacking case		Racking case	
	Longitudinal	Transverse	Longitudinal	Transverse	Longitudinal	Transverse
l_i (mm)	470	470	450	250	1050	360
a_i (mm)	340	140	130	94	214	142

Note: l_i = distance between the deck board supports. a_i = the distance between the point where the load is applied and the closest deck board support.

As an example, for the longitudinal racking test, the experimental curve corresponds to the loading of the test specimen until failure (below 2.0% of l_l = 1050, i.e. 21.0 mm). The peak U_t of 9.32 kN corresponds to the displacement recorded at failure, 18.54 mm.

Fig. 12 and Table 8 present all the ultimate load results of the laboratory tests. Table 8 also includes the suggested load limits ($\mathbf{P_t}$), for each loading scenario, which also ensures the elastic behaviour of the pallet (see Fig. 11).

The highest peak in Fig. 12 is related to the S: T-side test, which shows a high strength of the steel pallet for this case. In general, the results indicate that the metal pallet is more resistant on the transverse side. In fact, the mean value of U_t on the transverse side is 55.21 kN, whereas on the longitudinal side it is 24.342 kN. Overall, U_t ranges from ~9.9 to ~98.0 kN with a mean value of 39.77 kN.

One aspect regarding the different behaviour of the two sides can be checked by calculating the ratio of the $U_{t|T\text{-side}}/U_{t|L\text{-side}}$. For forklifting and stacking this ratio is very similar, with values of 2.46 and 2.22, respectively, whereas for the racking case, the ratio is 2.13. This is because the distance l_i for racking is greater than for the other cases, thus increasing its flexibility and reaching the ultimate load at a faster rate.

These results are consistent with the experimental test for deck board. In fact, this ratio, estimated as 1.88, is very close to the ratio for the whole pallet when considering all cases (i.e. 2.07).

Some figures have been gathered from the literature for comparison purposes. This is useful for providing an order of magnitude of the published work results because studies that are very similar have not been found in the literature. In [3], regarding paper pallets, static and dynamic carrying strength could reach about 10.0 kN. In [44], static load and bending load are estimated to be about 64.13 kN and 3.86 kN, respectively. The maximum load from the bending test for two wood-plastic composites ranges between 4.10 kN and 6.61 kN. The differences are mainly due to the geometry and material characteristics.

In general, in ISO 8611-2 [42], U_t values are provided without explicitly separating the ultimate load for the total pallet failure from a component failure. Also, the material used (probably wood) is not specified and a safety factor of 2.0 is defined in a very simplified way. The philosophy is that the optimum pallet is taken to be the one that sustains a higher load while having a lower mass in relation to the material that it is made of.

Finally, according to ISO 8611-1 [41] and ISO 8611-2 [42], the vertical displacements should be measured between blocks in the middle of the pallet's deck boards. Table 9 lists the performance limits and the results of the deformations obtained from the laboratory tests. A comparison between the FEM model, experimental results, and the standard [11] is shown.

In Table 9, $P_{t,a\%}$ is the recorded experimental load when the vertical displacement reaches a % of l_i, y_{max} is the maximum deformation at U_t. The maximum value relates to the point where the maximum deformation is expected following the scheme in Fig. 2. The maximum experimental deformations under U_t loads range between 23.42 and 34.62 mm, corresponding to the racking case and forklifting longitudinal cases. These results were expected given the numerical analyses. It is possible to see, for these three cases, high internal stresses, and "apparently" larger deflections (see red regions in Fig. 7).

This range is slightly larger than the maximum performance limit indicated in the code [11], i.e. 21.0 mm. However, the exact value of 21.0 mm is valid for wooden pallets, therefore results shown in Table 9 could provide new performance limits for metal pallets.

It is possible to see some differences between y_{max} given by the FEM model and experimental tests. This difference may result from the linear behaviour assumed by the FEM model, while the experimental tests consider the actual capacity of the material. Also, in the experimental tests the support and ground stiffness effect can alter the results.

4.3. Fatigue dynamic behaviour

The racking, forklifting, and stacking tests are not designed to evaluate the fatigue of the pallet in response to loading cycles applied during its lifespan. Additionally, those tests do not represent the dynamic loads generated by the real use of the pallets. This is particularly relevant in the case of forklifting actions where the rapid movements generate "dynamic" loads caused by the produced accelerations. To better understand the behaviour of the pallet under continuous forklifting actions under their lifespan, a fatigue test was performed using the setup used before (see Fig. 10).

The test specimen was subjected to 2.0×10^5 load sinusoidal cycles with an amplitude of ~6.0 kN, at a frequency of 5.0 Hz. This frequency was chosen because it is much higher than the possible frequency of a cycle-loading application in real life. Given the first natural frequency of the pallet of 20 Hz, evaluated experimentally, a steady-state amplitude response similar to that of the static displacement is expected.

Fig. 13 shows the measured vertical displacements in the longitudinal central line of the pallet for some of the loading cycles.

It is possible to see that the load-displacement loops are similar for each cycle (i.e. the cycles overlap between them), indicating a stable behaviour along with the full fatigue test. The maximum registered load is 5.95 kN, generating a maximum displacement amplitude of 1.39 mm, like that of the static displacement (1.45 mm). The pallet did not show any loss of strength after the fatigue test.

5. Environmental performance: Life cycle analysis (LCA)

As part of this work, an LCA study was carried out with the aim of identifying the main environmental impacts associated with the life cycle of the new proposed pallet made of galvanised steel (#Steel|New) and to compare them with those of reference pallets made of wood (#Wood|Ref1), plastic (#Plas-

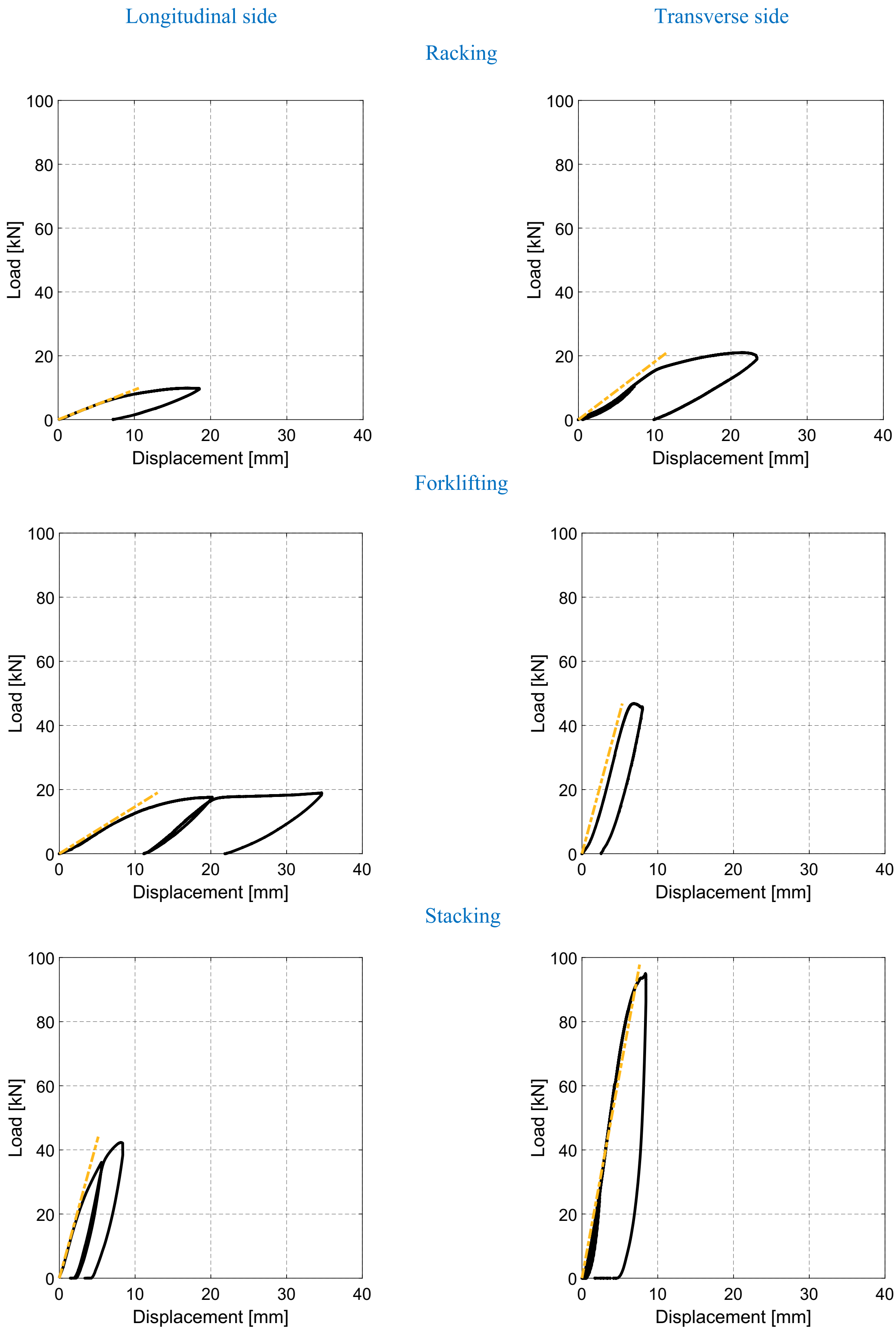

Fig. 11. Experimental (solid lines) and numerical (dashed lines) load-displacement curves for all tests performed on both sides.

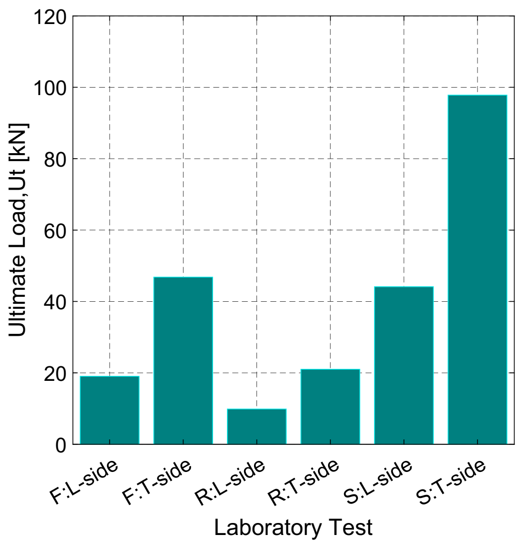

Fig. 12. Experimental test results for ultimate loads U_t (R = Racking, F = Forklifting, S = Stacking, T-side = Transverse side, L-side = Longitudinal side).

Table 8
Experimental results for each case.

Test measurement		Experimental results	
		U_t (N)	P_t (N)
Racking	T-side	21,000	10,500
	L-side	9866	4933
Forklifting	T-side	46,820	23,410
	L-side	19,030	9515
Stacking	T-side	97,800	48,900
	L-side	44,130	22,060

Note: U_t = Ultimate load for total pallet failure. P_t = Suggested test load limit to guarantee elastic behaviour.

tic|Ref2) and aluminium (#Alumin|Ref3). Typical photographs are presented in Fig. 14, while the main characteristics are summarised in Table 10. This analysis was performed using SimaPro software [55] in accordance with ISO 14040 [56] and ISO 14044 [57].

To perform this study, a "cradle-to-gate with options" model was developed, using real data for the production stage (extraction and processing of raw materials, transport to the factory and production) and building scenarios for the use stage (pallet replacement module) and end-of-life stage (transport and waste treatment module [62,63]). The remaining modules of the use stage (use and maintenance/repair) were not considered in this study due to lack of information. The declared unit was a pallet with a lifespan of 20 years. This declared unit was selected based on the main characteristics of these products and relevant information available in the literature. However, other declared units could have been used considering other characteristics of the pallets, such as the load capacity over the reference lifespan.

5.1. Inventory

With respect to the product stage of the metal pallets (#Alumin|Ref3 and #Steel|New), the inventory was prepared using available real data. The material inputs were modelled based on technical data sheets and data from suppliers and the distances for transporting materials were measured using Google Maps. The impacts associated with diesel consumption were considered for fuel transport, but the impacts of the manufacture and maintenance of vehicles were excluded. For electricity production, the energy mix from Portugal in 2014 (low voltage electricity - Portugal production mix) was considered [58]. The transport of waste generated in the production process to the management facility and its treatment processes, when available, were also considered. Data from previous LCA studies [19,23,59] were used to model the #Wood|Ref1 and #Plastic|Ref2.

Regarding the use stage, a service lifetime of 20 years was considered for #Steel|New (information provided by Portimpact company), while service lifetimes of 1.5 years, 10 years and 15 years were considered for #Wood|Ref1, #Plastic|Ref2 and #Alumin|Ref3, respectively [21]. To model this process, the production of replacement pallets, transport (for a scenario of 150 km) and treatment of the waste produced (incineration or recycling) were considered.

The end-of-life stage considered the transport of pallets to waste management operators, the recycling of metal pallets, the incineration of wooden pallets and incineration/landfill of plastic pallets, according to information from LCA studies of similar products [17]. For transport purposes, waste operators within a radius of 150 km were considered.

To supplement missing data, and compare and validate existing data, research literature and the "Ecoinvent v 3.6" database [58] were used. Table 11 and Table 12 summarise the inventory for the product and end-of-life stage, respectively.

5.2. Impact assessment

The life-cycle performance was assessed by using the midpoint approach in accordance with the CML–IA method - version 4.7 [60], i.e., abiotic depletion potential (ADP-elements and

Table 9
Vertical displacements and loadings.

Case	FEM model	Standard [11]				Experimental results		
	y_{max} (mm) [a]	l_i (mm)	6.0% l_i (mm)	2.0% l_i (mm)	0.70% l_i (mm)	$P_{t,6\%}$ (kN)	$P_{t,2\%}$ (kN)	y_{max} (mm) [a]
R: L-side	10.60	1050.0	63.0	21.0 [c]	7.35	N/R	N/R	18.54
R: T-side	11.60	360	39.30	7.2	4.59	N/R	17.76	23.42
S: L-side	5.14	450.0	27.00	9.0	3.15	N/R	37.53	8.44
S: T-side	7.61	250.0	15.00	5.0	1.75	N/R	26.59	8.50
F: L-side	12.99	–	–	20.0	7.0 [b]	N/R	17.63	34.62
F: T-side	5.32	N/A						7.99

Note: N/R = Not reached (failure has already occurred). N/A = Not available.
[a] y_{max} is calculated for U_t (Table 8).
[b] Maximum performance limit imposed by [11] for forklifting tests.
[c] Maximum performance limit imposed by [11] for racking tests.

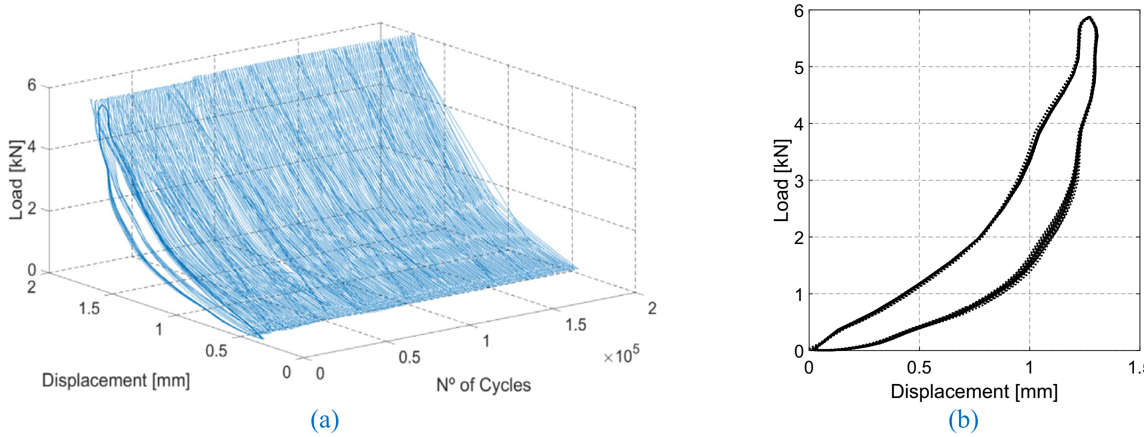

Fig. 13. Fatigue test of the pallet under a forklifting action along the transverse side: (a) Representation of cycles; (b) dynamic behaviour of the pallet.

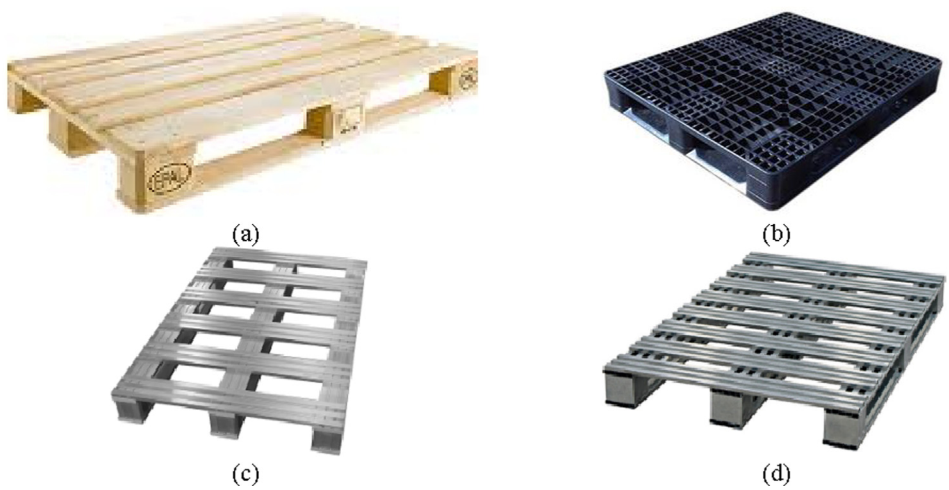

Fig. 14. Pallets: (a) #Wood|Ref1 - Wooden pallet; (b) #Plastic|Ref2 - Plastic pallet; (c) #Alumin|Ref3 - Universal welded pallet (aluminium); (d) #Steel|New - Universal welded pallet (galvanised steel).

Table 10
Main characteristics of the pallets under study.

Reference	Dimensions (mm)	Weight (kg)	Durability (years) [a]	Static load (kN) [b]
#Wood|Ref1	1200 × 800	25.0	1.5	15.0
#Plastic|Ref2		25.0	10	10.0
#Alumin|Ref3		11.4	15	20.0
#Steel|New		13.0	20	22.0

[a] Durability was established based on information provided by Portimpact company, for the steel pallet, and information available in the literature [21], for the wood, plastic, and aluminium pallets.
[b] Static load was established based on real experimental data, for the aluminium and steel pallets, and information available in the literature [19], for the wood and plastic pallets.

ADP-fossil resources), global warming potential (GWP), ozone depletion potential (ODP), photochemical oxidation creation potential (POCP), acidification potential (AP), and eutrophication potential (EP).

5.3. Product stage (cradle-to-gate)

The relative contribution of the inventory elements of the pallet product stage for the impact categories is presented in Fig. 15.

5.4. Comparative analysis (cradle-to-gate with options)

A comparative analysis of the environmental performance of the studied pallets for the more complete life cycle model (cradle-to-gate with options) is presented in Fig. 16.

Fig. 16 shows that for the metal pallets (#Alumin|Ref3 and #Steel|New) the product stage represents the greatest contribution to all the impact categories, which results from the very intensive consumption of resources during steel and aluminium production.

Table 11
Summary of the inventory of the product stage.

			Unit	#Wood|Ref1	#Plastic|Ref2	#Alumin|Ref3	#Steel|New
Production stage (Inputs)	Raw materials	Wood	kg	2.52E + 01	–	–	–
		Galvanised steel	kg	–	–	–	1.37E + 01
		Steel	kg	4.30E−01	–	–	–
		Aluminium	kg	–	–	1.14E + 01	–
		Polypropylene	kg	–	2.50E + 01	6.0E−02	–
	Subsidiary materials	Welding gas	m^3	–	–	2.0E−01	1.80E−01
		Finish - Paint for steel	kg	–	–	–	1.31E−01
		Finish - Solvent-based ink	kg	4.20E−02	–	–	–
		Lubricant	l	–	–	3.07E−03	2.74E−03
	Energy	Electricity from the grid	kWh	7.00E−01	1.41E + 01	3.07E + 00	3.07E + 00
		Heat - Natural gas	MJ	6.10E + 00	–	–	–
		Light fuel oil	l	1.70E−02	–	–	–
		Diesel	l	–	6.30E−01	–	–
	Raw materials' transport	Truck	tkm	–	–	5.26E−01	1.43E + 00
	Subsidiary materials' transport	Light truck	tkm	–	–	1.66E−01	1.76E−01
Production stage (Outputs)	Waste	Steel shavings and chips	kg	–	–	–	7.80E−01
		Aluminium shavings and chips	kg	–	–	3.10E−01	–
		Wood shavings	kg	2.0E−01	–	–	–
	Waste transport	Light truck	tkm	–	–	1.83E−03	4.60E−03

Table 12
Summary of the inventory of the use and end-of-life stages.

				Unit	#Wood|Ref1	#Plastic|Ref2	#Alumin|Ref3	#Steel|New
Use stage	Replacement	No. of lifetime replacements		–	13	2	1	0
		Inputs	New pallet	kg	3.25E + 02	5.0E + 01	1.14E + 01	–
		Outputs	Pallet waste	kg	3.25E + 02	5.0E + 01	1.14E + 01	–
			Transport - Light truck	tkm	4.88E + 01	7.50E + 00	1.71E + 00	–
End-of -life stage	Waste transport		Light truck	tkm	3.75E + 00	3.75E + 00	1.71E + 00	2.08E + 00
	Waste treatment		Incineration	kg	2.50E + 01	1.35E + 01	–	–
			Landfill	kg	–	1.15E + 01	–	
			Recycling	kg	–	–	1.14E + 01	1.39E + 01

Regarding the reference pallets (#Wood|Ref1 and #Plastic|Ref2), it is possible to see that replacing the pallets during the use stage represents a major contribution for all the impact categories. Note that in the case of #Wood|Ref1 and #Plastic|Ref2, thirteen and two complete replacements, respectively, are necessary during the defined lifetime. By contrast, for the galvanised steel pallet (#Steel|New), replacement during the defined lifetime is not necessary. Regarding the end-of-life stage, a desirable negative contribution is obtained for the metal pallets, thanks to the high recyclability of the materials.

Finally, taking into account the product stage and other stages of the life cycle, the galvanised steel pallet under study is the solution offering best performance for all impact categories, while the plastic pallet (#Plastic|Ref2) performs worst for most of the impact categories.

6. Conclusions

This paper has focused on the design and multi-analysis of modular steel pallets that combine blocks and deck boards to produce different configurable structures. A combined numerical and experimental approach was used to validate the performance of these pallets under transportation (dynamic forklifting) and stationary (racking, stacking) conditions. An LCA was also carried out to identify the main environmental impacts associated with the life cycle of steel pallets, comparing the results with those obtained for corresponding solutions made of wood, plastic, or aluminium.

The following main conclusions emerge from this work:

- 3D FEM models proved to be useful to estimate the stresses and deformations for different load conditions. The general compressive resistance of the whole pallet supported by blocks is ~480.0 kN. The most critical case was found for the racking test with stress > 140 MPa.
- Laboratory tests, used to validate the models, provided new ultimate and test loads, for total pallet failure and performance limits. The ultimate load ranges between 9.9 and 98.0 kN, the $U_{t|T\text{-side}}/U_{t|L\text{-side}}$ ratio ranges between 2.1 and 2.4, and the maximum deformation registered is 0.34.62 mm. Also, the dynamic fatigue test shows a good performance by the new galvanised steel pallets. Therefore, for a specific analysis of metal pallets, the present values and design procedures can be used to update some of the existing codes [26,42].
- A comparative LCA study based on a "cradle-to-gate with options" model suggests that galvanised steel pallets perform better than their wood, plastic, and aluminium counterparts, mainly due to high recyclability and less need of repairing or replacement during the defined service lifetime.

Finally, this paper demonstrates that galvanised steel pallets perform satisfactorily in terms of resistance and stiffness. Additionally, given the different demands of dimensions and weight, the development of pallets with modular technology could prove to be a good choice to fulfil the functional requirements for different industries.

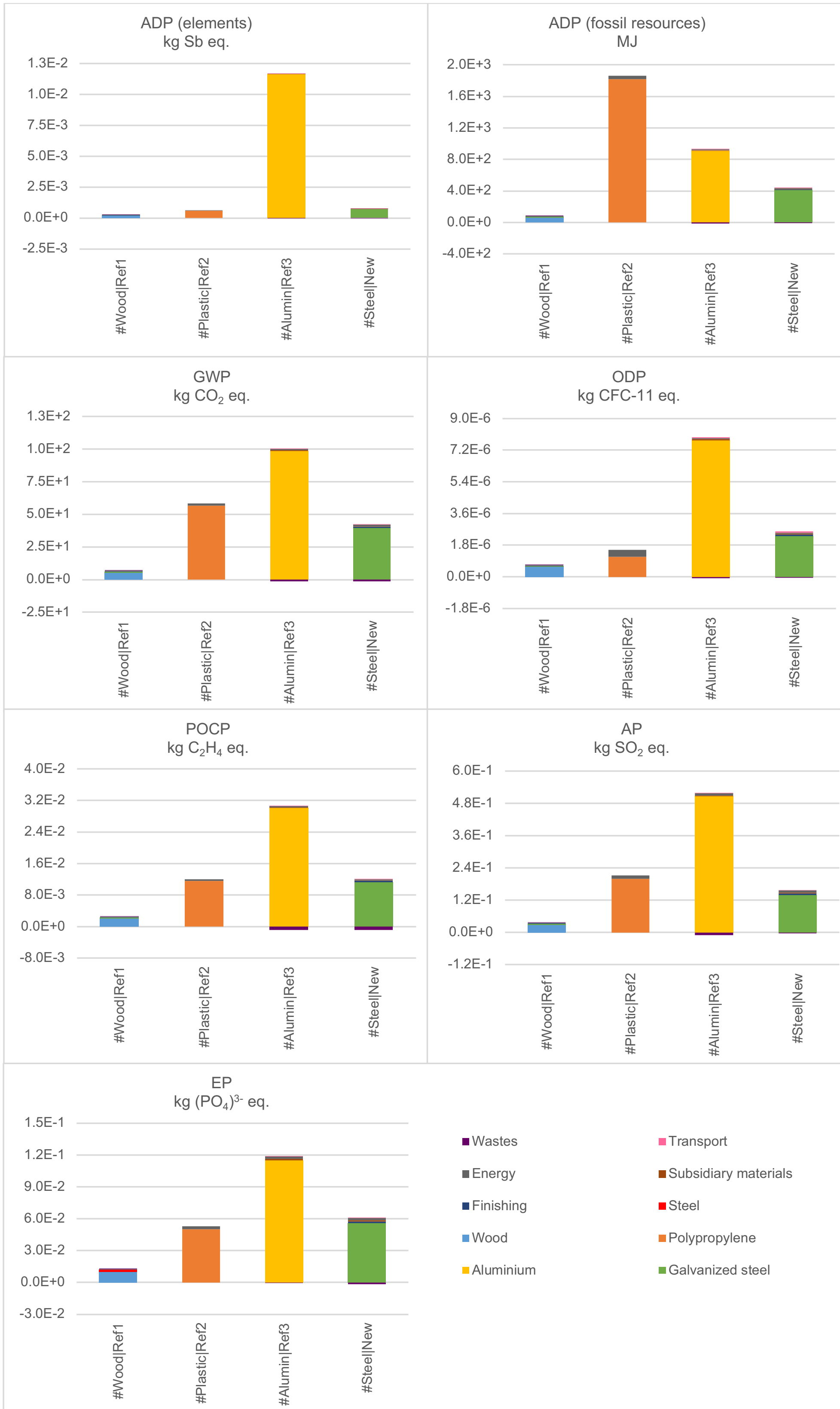

Fig. 15. Comparative impact assessment of the different inventory elements (product stage only) for the pallets under study: #Wood|Ref1; #Plastic|Ref2; #Alumin|Ref3; and #Steel|New.

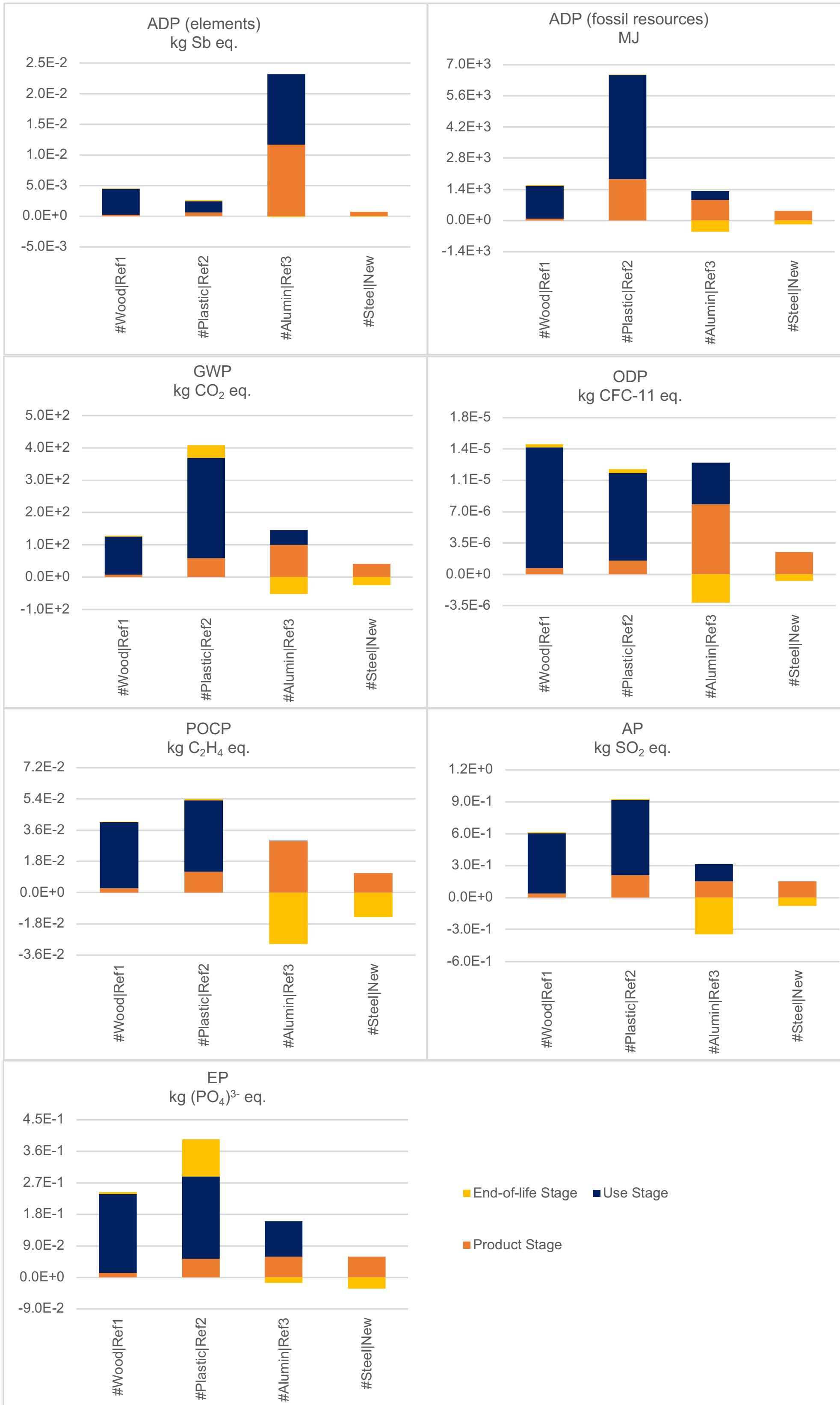

Fig. 16. Comparative environmental performance of the studied pallets (cradle-to-gate with options): #Wood|Ref1; #Plastic|Ref2; #Alumin|Ref3; and #Steel|New.

Declaration of Competing Interest

The authors declare that they have no known competing financial interests or personal relationships that could have appeared to influence the work reported in this paper.

Acknowledgements

This work was carried out under POCI-01-0247-FEDER-033369 (QuickPALLET). Project funded by Portugal 2020 through COMPETE 2020. The authors would like to thank Óscar Lopez for providing some analyses and data and David Tadeu for performing the laboratory tests at Itecons (Coimbra, Portugal).

References

[1] S. Alvarez, A. Rubio, Compound method based on financial accounts versus process-based analysis in product carbon footprint: A comparison using wood pallets, Ecol. Ind. 49 (2015) 88–94.
[2] U. Buehlmann, M. Bumgardner, T. Fluharty, Ban on landfilling of wooden pallets in North Carolina: an assessment of recycling and industry capacity, J. Cleaner Prod. 17 (2) (2009) 271–275.
[3] National Wooden Pallet and Container Association (NWPCA). Accessed on 10/2021. https://www.palletcentral.com/
[4] H. Quesada-Pineda, S. Sanchez-Gomez, P.A. Araman, A quantitative study of the U.S. wood pallet industry based on supply chain management practices, J. Appl. Packaging Res. 6 (1) (2012) 1–26.
[5] V. Elia, M.G. Gnoni, Designing an effective closed loop system for pallet management, Int. J. Prod. Econ. 170 (2015) 730–740.
[6] R. Ng, C.W.P. Shi, H.X. Tan, B. Song, Avoided impact quantification from recycling of wood waste in Singapore: an assessment of pallet made from technical wood versus virgin softwood, J. Cleaner Prod. 65 (2014) 447–457.
[7] P.A. Araman, M.F. Winn, M.F. Kabir, X. Torcheux, G. Loizeaud, Pallet cant soundness at Appalachian sawmills and marketing recommendations, in: 30th Hardwood Symposium Proceeding, Tennessee, USA, May 30 - June 1, 2002, 88–94.
[8] S. Hassanzadeh Amin, H. Wu, G. Karaphillis, A perspective on the reverse logistics of plastic pallets in Canada, J. Remanuf. 8 (3) (2018) 153–174.
[9] P. Hamner, M. White, P. Araman, The effect of curve sawing two-sided cants from small-diameter hardwood sawlogs on lumber and pallet part yields, Forest Prod. J. 56 (10) (2006) 80–85.
[10] P.A. Araman, M.F. Winn, M.F. Kabir, X. Torcheux, G. Loizeaud, Unsound defect volume in hardwood pallet cants, Forest Prod. J. 53 (2) (2003) 45–49.
[11] M.S. White, P. Hammer, Pallets move the World - The case for developing system-based designs for unit loads, Forest Prod. J. 55 (3) (2005) 8–16.
[12] F. Tornese, A.L. Carrano, B.K. Thorn, J.A. Pazour, D. Roy, Carbon footprint analysis of pallet remanufacturing, J. Cleaner Prod. 126 (2016) 630–642.
[13] S. Alanya-Rosenbaum, R. Bergman, B. Gething, Developing procedures and guidance for performing an environmental assessment of us wooden pallets, WIT Trans. Ecol. Environ. 215 (2018) 37–45.
[14] J. Terno, G. Scheithauer, U. Sommerweiß, J. Riehme, An efficient approach for the multi-pallet loading problem, Eur. J. Oper. Res. 123 (2) (2000) 372–381.
[15] C.W. Chen, The development of a new paper pallet machine, Proc. Eng. Technol. Innov. 6 (2017) 17–22.
[16] A.L. Carrano, B.K. Thorn, H. Woltag, Characterizing the carbon footprint of wood pallet logistics, Forest Prod. J. 64 (7) (2014) 232–241.
[17] A.M. Bilbao, A.L. Carrano, M. Hewitt, B.K. Thorn, On the environmental impacts of pallet management operations, Manage. Res. Rev. 34 (11) (2011) 1222–1236.
[18] S.K. Anil, J. Ma, G.E. Kremer, C.D. Ray, S.M. Shahidi, Life cycle assessment comparison of wooden and plastic pallets in the grocery industry, J. Ind. Ecol. 24 (4) (2020) 1–16.
[19] V. Kočí, Comparisons of environmental impacts between wood and plastic transport pallets, Sci. Total Environ. 686 (2019) 514–528.
[20] S. Kurisunkal, A. Philip, Environmental analysis of pallets using life cycle analysis and multi-objective dynamic programming, A Thesis in Industrial Engineering, Pennsylvania State, University College of Engineering, USA, 2010.
[21] A.M. Bilbao, Environmental impact analysis of alternative pallet management systems, Dissertation for Master of Science Degree, Department of Industrial & Systems Engineering, Kate Gleason College of Engineering, Rochester Institute of Technology, USA, 2011.
[22] Edge Environment Pty Ltd, Report for Range International: Pallet Life Cycle Assessment and Benchmark, 2017.
[23] C.M. Gasol, R. Farreny, X. Gabarrell, J. Rieradevall, Life cycle assessment comparison among different reuse intensities for industrial wooden containers, Int. J. Life Cycle Assess. 13 (5) (2008) 421–431.
[24] J. Bengtsson, J. Logie, Life cycle assessment of one-way and pooled pallet alternatives, The 22nd CIRP conference on Life Cycle Engineering, Australia, Procedia CIRP 29 (2015) 414–419.
[25] A.L. Carrano, J.A. Pazour, D. Roy, B.K. Thorn, Selection of pallet management strategies based on carbon emissions impact, Int. J. Prod. Econom. 164 (2015) 258–270.
[26] European Committee for Standardization (CEN), Eurocode 3 – Design of steel structures – Part 1-3: General rules – Supplementary rules for cold-formed members and sheeting, BS EN 1993-1-3:2006, Brussels, Belgium, 2006.
[27] European Committee for Standardization (CEN), Eurocode 3 – Design of steel structures – Part 1-1: General rules and rules for buildings, BS EN 1993-1-1:2005, Brussels, Belgium, 2005.
[28] European Committee for Standardization (CEN), Eurocode 3 – Design of steel structures – Part 1-5: General rules – Plated structural elements, BS EN 1993-1-5:2006, Brussels, Belgium, 2006.
[29] M.P. Talele, A.J. Keche, Design optimization and simulation study of the engine transportation metal pallet for stationary and movable condition, Int. J. u- and e- Service, Sci. Technol. 8 (2015) 219–230.
[30] H. Yaman, A. Şen, Manufacturer's mixed pallet design problem, Eur. J. Oper. Res. 186 (2008) 826–840.
[31] F. Gzara, S. Elhedhli, B.C. Yildiz, The pallet loading problem: Three-dimensional bin packing with practical constraints, Eur. J. Oper. Res. 287 (2020) 1062–1074.
[32] J.W. Clarke, T.E. McLain, M.S. White, P.A. Araman, Evaluation of metal connector plates for repair of wood pallet stringers, Forest Prod. J. 43 (10) (1993) 15–22.
[33] M.F. Kabir, D.L. Schmoldt, P.A. Araman, M.E. Schafer, S.M. Lee, Classifying defects in pallet stringers by ultrasonic scanning, Wood Fiber Sci. 35 (3) (2003) 341–350.
[34] K. Adamakos, S. Sesana, I. Vayas, Interaction between pallets and pallet beams of steel storage racks in seismic areas, Int. J. Steel Struct. 18 (3) (2018) 1018–1034.
[35] E. Safronov, A. Nosko, A method to determine allowable speed for a unit load in a pallet flow rack, Sciendo 13 (2019) 80–85.
[36] S.N.R. Shah, N.H. Ramli Sulong, M.Z. Jumaat, M. Shariati, State-of-the-art review on the design and performance of steel pallet rack connections, Eng. Fail. Anal. 66 (2016) 240–258.
[37] Z. Lyu, J. Zhang, N. Zhao, Q. Xiang, Y. Song, J. Li, A comparative study on the performance of FEM, RA and ANN methods in strength prediction of pallet-rack stub columns, Int. J. Steel Struct. 20 (2020) 1509–1526.
[38] S.N.R. Shah, N.H. Ramli Sulong, M. Shariati, R. Khan, M.Z. Jumaat, Behaviour of steel pallet rack beam-to-column connections at elevated temperatures, Thin-Walled Struct. 106 (2016) 471–483.
[39] SolidWorks, software version 27, Dassault Systèmes SolidWorks Corporation, USA, 2019.
[40] Wolfram Mathematica 12, software version number 12.0, Wolfram Research, Inc., 2019.
[41] Test methods (2011).
[42] International Organization for standardization (ISO), ISO 8611-2:2011 – Pallets for materials handling – Flat pallets – Part 2: Performance requirements and selection of tests, 2011.
[43] International Organization for standardization (ISO), ISO 8611-3:2011 – Pallets for materials handling – Flat pallets – Part 3: Maximum working loads, 2011.
[44] E. Soury, A.H. Behravesh, E. Rouhani Esfahani, A. Zolfaghari, Design, optimization and manufacturing of wood-plastic composite pallet, Mater. Des. 30 (2009) 4183–4191.
[45] J.W. Clarke, Pallets 101: Industry overview and wood, plastic, paper & metal options, PreShipment Testing, 1-9, 2004.
[46] A. Trevisan, E. Iaccheri, A. Fabbri, A. Guarnieri, Pallet standards in agri-food sector: a brief survey, J. Agric. Eng. 220 (2014) 90–95.
[47] S.J. Chavan, R.N. Patil, N.A. Dhanrale, Design and static stress analysis of returnable pallet for steel wheel, Int. J. Sci., Eng. Technol. Res. 5 (6) (2016) 2101–2103.
[48] S. Malasri, A. Pourhashemi, P. Aung, M. Harvey, R. Moats, Water absorption of wooden pallets, Int. J. Appl. Sci. Technol. 2 (2012) 1–10.
[49] European Committee for Standardization (CEN), Continuously hot-dip coated steel flat products – Technical delivery conditions, EN 10292:2007, Brussels, Belgium, 2009.
[50] J. Li, Y.Y. Qiu, H.D. Wang, Z.X. Wang, Estimation of the strength coefficient and strain hardening exponent from monotonic tensile properties of steels, Int. J. Steel Struct. 19 (2019) 1951–1968.
[51] J.W. Clarke, M.S. White, P.A. Araman, Comparative performance of new, repaired, and remanufactured 48- by 40-inch GMA-style wood pallets, Forest Prod. J. 55 (12) (2005) 83–88.
[52] J.W. Clarke, T.E. McLain, M.S. White, P.A. Araman, Reinforcement of wood pallets with metal connector plates, Forest Prod. J. 43 (10) (1993) 70–76.
[53] A.L. Rojas, S.L. Chavarría, M.M. Elizondo, V.V. Kalashnikov, A mathematical model of elastic curve for simply supported beams subjected to a concentrated load taking into account the shear deformations, Int. J. Innov. Comput., Inform. Control 12 (2016) 41–54.
[54] HBM Catman AP, software version 4.03, HBM Company, 2019.
[55] SimaPro software, PRé Consultants bv 1990-2020, Release 9.1.0.11.
[56] International Organization for Standardization (ISO), ISO 14040 - Environmental management: Life Cycle Assessment - Principles and framework, 2006.
[57] International Organization for Standardization (ISO), ISO 14044/Amd1 - Environmental management - Life cycle assessment - Requirements and guidelines, 2006.

[58] E.M. Ruiz, L. Valsasina, F. Brunner, A. Symeonidis, D. FitzGerald, K. Treyer, G. Bourgault, G. Wernet, Documentation of changes implemented in ecoinvent database v3.5, Ecoinvent, Zürich, Switzerland, 2018.
[59] I. Deviatkin, K. Musharof, E. Ernst, M. Horttanainen, Wooden and plastic pallets: A review of life cycle assessment (LCA) studies, Sustainability 11 (20) (2019) 1–17.
[60] PRé, SimaPro Database Manual Methods Library, vol. 4.14.2, 2019.
[61] AutoCAD (2010) Version 2010. Autodesk, Inc., 2010.
[62] CEN - European Committee for Standardization, EN 15804 - Sustainability of construction works - Environmental product declarations - Core rules for the product category of construction products, 2012.
[63] M. Yazdani, K. Kabirifar, B.E. Frimpong, M. Shariati, M. Mirmozaffari, A. Boskabadi, Improving construction and demolition waste collection service in an urban area using a simheuristic approach: A case study in Sydney, Australia, J. Clear Prod. 280 (2021) 1–17.